

## EXPERIMENTAL QUANTIFICATION OF THE PLANAR DROPLET SIZING TECHNIQUE ERROR FOR MICRO-METRIC MONO-DISPERSED SPHERICAL PARTICLES

Lucio ARANEO \*, Raul PAYRI °

\* Politecnico di Milano, Dipartimento di Energia, Via La Masa 34, 20156 Milano, Italy  
° CMT Motores Termicos, Universidad Politecnica de Valencia, Camino de Vera , Valencia 46022

### ABSTRACT

The Planar Droplet Sizing (PDS) technique was used to measure the ratio of the elastic scattered light to the fluorescence signal emitted by fluorescent monodispersed microspheres homogeneously suspended in water and illuminated by a pulsed laser sheet. Three cells with different known particle concentrations, illuminated with different laser sheet positions were tested. Deviation from a constant value of the two signals ratio allows to verify in which conditions the PDS hypotheses don't hold any more and the technique should not be applied to size the particles; the results evidences that in a dense environment secondary light scatter is dramatically affecting the results. A full analysis of the error origins and propagation allows quantitative estimation of the technique precision as a function of the used system geometry and other experimental parameters. Overall results are expected to be directly referred to real sprays.

### INTRODUCTION

The experimental characterisation of sprays is of crucial importance to many technical applications [3]: for example most of liquid fuels are sprayed to evaporate and mix with the air for the subsequent combustion, and this process is strongly influenced by the spray characteristics; also for CFD purposes it is fundamental to have the spray data to initialize and later to check the simulations. Some of these investigated characteristics are: spray shape and structure (full or hollow cone, fan, opening angle, length), break-up characteristics, liquid phase description (mass and surface distribution, particles/droplet velocity and size), gas and vapour phases composition and velocity, temporal evolution of all these parameters in case of an unsteady spray.

External macroscopic parameters are easily measured since decades with well established, techniques, but many other parameters regarding the internal and microscopic description of the spray are still difficult to investigate

Three main problems are:

- the spray optical opacity, that means difficult optical access to the internal parts of it with non intrusive techniques

- the enormous number of droplets: a typical engine spray of 50 milligrams is composed by millions of droplets; not being possible to describe all of them, it is necessary to give some average indicators, most of them

being function of the time and three-dimensional space position.

- the required instrument dynamic range: if many droplet characteristics are surface or volume dependent (evaporation, gas adsorption, light scattering, fluorescence, mass, inertia), a wide droplet size distribution is a big challenge for linear instruments.

For an extensive review of different sizing techniques, many specialised books [e.g. 7, 13, 14] are available, but only few of them can be applied to sprays, like Phase Doppler Anemometry PDA [1], and diffraction sizing, (the instrument is often called Malvern from the name of a company).

Often the analogy between a spray and a gas jet [2] has been helpful in understanding and describing the spray in its more diluted region, but the dens core behave differently and is still an issue. If the spray is so dense that the beam transmission falls below 85%, multiple scattering problems arise [15]; correction is possible with some limitations up to a few percent of transmission.

Some authors had to open the spray by a mechanical device to see its inside parts [12]; X-rays analysis seems to be promising [4], but at the moment it is at the experimental and development stage, and commercial instruments are not yet available.

The Planar Droplet Sizing (PDS) technique seems to be an interesting solution to investigate some spray characteristics, particularly attractive for fast transient sprays. The idea, introduced by [15], is that, when a droplet is illuminated by an appropriate light source, the

elastically scattered light intensity is proportional to the droplet surface, while the fluorescent emission is proportional to the droplet volume, so that the ratio of the two intensities is proportional to the droplet diameter; from a group of droplet the intensity ratio is therefore proportional to the Sauter mean diameter (SMD). In this way PDS needs only to be calibrated in one point of the spray, and then the results could be extended to a whole area illuminated by a laser sheet and photographed. But if one or both signals undergo partial extinction or multiple scattering with different intensity, then the proportion in the measured signal doesn't hold any more.

In the present work we use a simple experiment to highlight and quantify some limits of the PDS and their origin. Measurements are performed in a known environment, constituted by fluorescent particles of known size, suspended in water with known and on average homogeneous concentration; in these conditions, if the technique holds, the ratio between the scattered and the fluorescent signals should be constant. Three different particle concentration were chosen, allowing different intensity of signal attenuation and secondary scattering. The ratio of the scattered and fluorescent signals could be calculated for different experimental conditions. The results show that the ideal linearity between signals ratio and particle diameter holds only in a limited range of experimental conditions.

The original idea of the PDS is that, when a spray or a cloud of fluorescent particles is illuminate by a laser sheet, under certain hypothesis, the intensity of the elastically scattered light, that can be predicted by the Mie theory, is proportional to the total droplet surface  $S_{Mie} = C_{Mie} \sum D_i^2$ , while the Laser induced fluorescence intensity is proportional to the total volume  $S_{LIF} = C_{LIF} \sum D_i^3$ , where  $C_{Mie}$  and  $C_{LIF}$  are some constant depending on the optical set-up, so that the simple ratio between two images taken at different wavelength gives

$$\frac{S_{LIF}}{S_{Mie}} = \frac{C_{LIF}}{C_{Mie}} \cdot \frac{\sum D_i^3}{\sum D_i^2} \propto SMD$$

so from the ratio of the images, and by knowing the SMD in only one location, the SMD in the whole image can be obtained. [5, 6, 9].

The technique could be self-compensating: any inhomogeneity of the laser sheet, of the imaging system and even in the environment affecting the two signals should be compensated thanks to the ratioing of the two signals.

The necessity to verify the PDS for sprays had already been evidenced by many authors, but it is not an easy task because of the inherent difficulty in having a spray of known characteristics. So some authors were able to investigate the behaviour of a single or a stream of spherical droplets obtained by a droplet generator. [5] verified numerically that the signal ratio shows minimum deviation from linearity for droplet diameter between 20 and 300 microns, with some other constraint for the liquid opacity and fluorescence characteristics. [11] verified experimentally the signal – diameter

relationship for few monodispersed droplet streams. Of course the fluorescence emission could be saturated by excessive excitation intensity, neither can the emission be proportional to the droplet volume if the exciting light is attenuated on the droplet surface and can not reach the whole internal droplet volume with nearly constant intensity.

From droplets smaller than 20 microns, the angular oscillation in the scattered signal becomes clearly visible.

## EXPERIMENTAL SET-UP

To build a physical system that for the measurement techniques acts like a spray, that is droplets in a gas, but whose characteristics are known with sufficient accuracy, the choice was to use spherical fluorescent particles of known diameter dispersed in water. The particle chosen have a diameter of 16 microns  $\pm 10\%$  (Duke Scientific Fluorescent Polymer Dry Microspheres, catalogue number 36-4), refractive index 1.59 at 589 nm; they are doped with Nile red (dye concentration is not available) that exhibits a Stoke shifts of 70 nanometres, with maximum efficiency in the green absorption, so when the particles are excited at 532 nm by a YAG laser, they emit in the red region of the visible spectrum. The particle density is 1050 kg/m<sup>3</sup>, so in water they slowly dive, but they could also float because of water surface tension. The particles were dispersed in three identical rectangular cell (Hellma large cell, cat. number 740.000-OG) with 100 cm<sup>3</sup> nominal volume, with internal dimension 44x34.5x97h millimetres, filled with 80 grams of distilled water and nominal 3, 9 and 27 mg of particles respectively. Table 1 shows a summary of the cells contents and characteristics; a fourth cell with only water was used for calibration purposes.

The measured extinction efficiency [8], for the particles in our set-up is  $Q_{ext}=0.76 \pm 6\%$ , and the optical thickness  $\tau$  for the laser sheet crossing the cells is calculated as

$$\tau = Q_{ext} \rho \sigma_{geom} Z \quad (Z=44 \text{ mm, see figure 1})$$

and is given in table 1. Before each set of experiments, the cell to test was conditioned by an ultrasonic bath cleaner, to separate possible particles aggregates, and kept on a magnetic stirrer during the tests to avoid particle segregation and to keep constant homogeneous particle dispersion.

The light source is a YAG laser (continuum Surelite II) equipped with second harmonic generator for 532 nm wavelength and operated at 10 Hz of pulse frequency. An optical head with a combination of cylindrical and spherical lenses allows to shape the laser beam like a slightly divergent fan with vertical height of 20 cm and thickness of 3 cm just before the cell position, where a large slit (25x3 mm) acts as spatial filter and allows only the central portion of the laser sheet to illuminate the cell, thus avoiding the original Gaussian intensity

profile. This feature is very helpful when the image acquisition system used has a limited dynamic range.

To record the images, a CCD digital camera (PCO Sensicam, 12 bit dynamic range in black and white, 1280x1024 pixels) was used, mounted with the optical

axis perpendicular to the laser sheet, and synchronized with the laser synchronization system. The objective had a maximum aperture  $A = F/3.5$ .

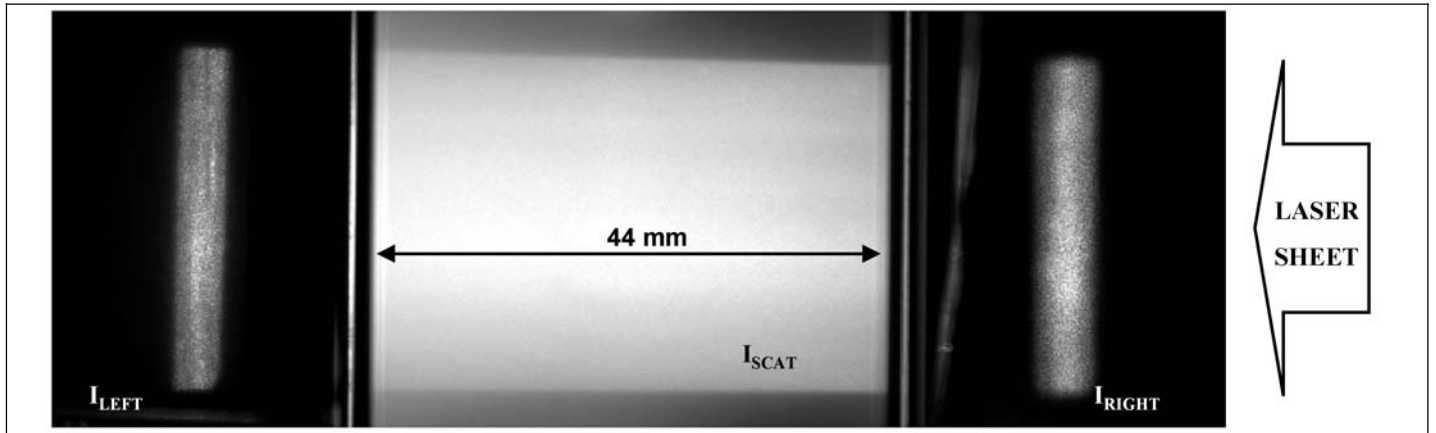


Figure 1. Photo (green filter) of the 27mg suspension inside the cell, with the images of the laser sheet profile used for reference on the right, and profile after extinction on the left.

Table1: Cell characteristics.

Nominal weight of the particles (mg)	empty	3 mg	9 mg	27 mg
Estimated accuracy on the weight (mg)		$\pm 0.5$ mg	$\pm 0.5$ mg	$\pm 0.5$ mg
Estimated weight by extinction measurement, (mg)		$2.47 \pm 0.05$	$9 \pm 0.17$	reference
Estimated particles number density ( $p/mm^3$ )		13.73	49.98	149.95
Calculated extinction coefficient	0	0.092	0.337	0.998

Table2: Optical set-up characteristics, common to all cells.

Size of the illuminated particle suspension (the size in pixels changes slightly with different Optical Depth )	mm	44 hor, 27 ver, 3 thickness
	Pixels	$550 \pm 5$ hor, $340 \pm 3$ ver
Suspension thickness between laser sheet and objective (OD)	mm	0, 4, 8, 12, 16, 20, 24, 28

Before the cell, a 4%-96% beam-splitter positioned at  $45^\circ$  was used to monitor the laser sheet: with adequate attenuation, an image of the sheet profile was recorded together with each picture. On the exit side of the laser sheet from the cell, another screen at  $45^\circ$  was used to measure the attenuation after the microspheres suspension.

A green band-pass filter ( $532 \pm 5$  nm) was placed in front of the objective, for the elastic scatter detection, while for the fluorescence a long-pass red filter (cut-off length 590nm) was placed in front of the cell only, to allow for the laser sheet monitoring.

Figure 1 shows a typical acquired image. The illuminated part of the cell is in the centre; on the right side the calibration sheet profile, on the left side the attenuated sheet profile. Note the laser sheet vertical

spread due both to its original optical divergence and to the secondary scattering.

The cell with the stirrer are mounted on a manual linear guide, to move only the cell along the camera optical axis, so that the standing laser sheet could enter the cell at different position. The illuminated particles are seen by the camera through the same liquid and particle suspension whose thickness, indicated as Optical Depth OD, can be chosen from zero (the illuminated particles are just beyond the cell wall) to 28 millimetres by traversing the cell. Although the laser sheet distance to the camera doesn't change, the different thickness of crossed water, because of its refractive index, leads to a slight change in the visualised image dimension, and to a displacement of the focused plane inside the cell, that reaches 7 mm

maximum, that is similar to the depth of focus of the camera, and therefore is negligible.

## DATA ACQUISITION AND PROCESSING

A preliminary system characterisation was performed to identify and reduce the error sources. The images of scattering and fluorescence were acquired in different moments after switching the two coloured filter: this gives the advantage of preserving the same identical optical alignment, except for the different thickness of the green and red filters, so that the image superposition quite immediate and doesn't need any kind of resizing or de-warping. The disadvantages are mainly that the particles are not in the same position, and that the laser sheet is not the same. For the particles, it was decided to work on average images, so that most of the images used are an average of 100 or 256 different laser shots. For the laser time variation, all processing are subsequently referred to the calibration sheet profile, indicated as  $I_{Right}$  in Figure 1.

Note that the laser sheet shows spatial variations: the expected intensity attenuation from right to left would be caused mainly by the laser attenuation from the particles and by the slight sheet divergence. The increase of intensity in the same direction, also appreciable as a spread in the vertical direction, is attributed to multiple scattering. The vertical intensity variations of the laser sheet profile are mainly due to its originally Gaussian profile, inhomogeneities, optical defects and variations of the laser sheet peak position showing both a long period temporal drift due probably to thermal variation and random shot-to-shot variations. Since these vertical variations in the laser sheet profile are not important, the results will be processed after vertical averaging, to study the more important variations in the horizontal direction.

## DATA REDUCTION

Each image is acquired already as an average from 256 exposures; this operation is directly performed by the acquisition software. From each images the following values are obtained:

$I_{Right}$ : is a scalar value representing the average intensity of the illuminating laser sheet, calculated over a narrow vertical rectangle. It is used for data equalization.

$I_{Left}$ : is a scalar value representing the average intensity of the residual laser sheet, calculated over a narrow vertical rectangle. It is used to measure obscuration.

$I_{Scat}(pixel)$ : is a vector representing the average intensity of the laser sheet in the vertical direction as a function of the horizontal position expressed in pixels.

The indexes Red or LIF, and Green or Mie, refer respectively to fluorescence and elastic scattering.

Figure 2 shows the profiles of  $I_{Scat}$ , for the red  $I_{LIF}$  and green colours  $I_{Mie}$ , different concentration, parametrised by the optical depth.

The fluorescence profiles behave as expected: at 3 mg the intensity decreases slightly in the direction of laser propagation, both for attenuation by the particles and the sheet divergence; no evident decrease is seen at different optical depth. The 9 and 27 mg show clearly the intensity decrease both with the laser penetration and with the optical depth.

The elastic scattering (Mie) profiles show the expected profile only at the lower 3 mg concentration; the signal is slightly irregular mostly because of unavoidable reflexes caused by the cell's walls. At 9 and 27 mg there is the inversion from the expected behaviour, in the direction of laser propagation from right to left, the scattered intensity increases, and the effect is strongly accentuated by the optical depth; this is attributed mostly to the multiple scattering that diffuses the laser sheet giving to it a divergent angle. So on the laser right side, where the laser has travelled only a short path and the secondary scattering is not directed towards the camera, the photographed intensity decreases with the optical depth, as expected because of the obscuration, while on the left side more light is directed toward the camera after multiple scattering by the particles standing in the thickness of the optical depth (OD) between the cell frontal wall and the laser sheet.

From the data shown in figure 2, the SMD is then calculated in function of the horizontal pixel position as:

$$\begin{aligned} SMD(pixel) &= \frac{I_{Scat,Red(pixel)} / I_{Right,Red}}{I_{Scat,Green(pixel)} / I_{Right,Green}} = \\ &= \frac{I_{Scat,Red(pixel)}}{I_{Scat,Green(pixel)}} * \frac{I_{Right,Green}}{I_{Right,Red}} \end{aligned}$$

where the last factor is an equalisation coefficient that corrects the laser temporal variations.

The result is a vertically and time averaged SMD, function of the pixel position, expressed in arbitrary unities, that could be reverted to dimensional diameter results after calibration in one point. In this experiment the real diameter is known and constant, so that the important result is the relative dispersion of the calculated SMD as a function of the used parameters, which are distance in pixels, optical depth OD and particle concentration. In ideal conditions the measures SMD should be constant, but the result reported in figure 3 shows a quite different behaviour.

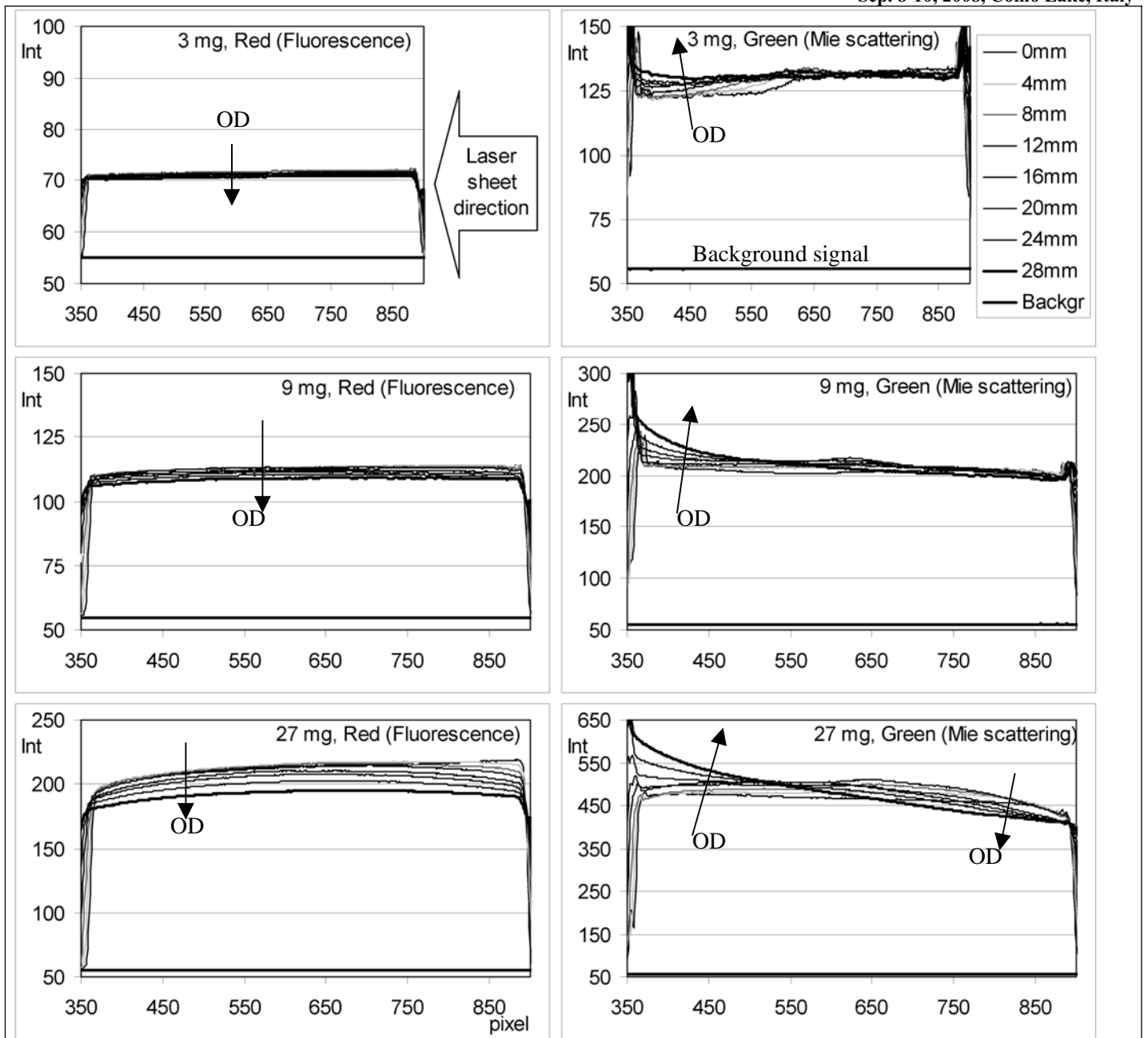


Figure 2: Raw profiles of  $I_{Scat}$  (not normalised by  $I_{Right}$ ), for the fluorescence and elastic (Mie) scattering, 3, 9 and 27mg of particle in the cell, parametrised by the optical depth. Laser sheet entering from the right side. Background noise intensity  $\cong 55$ ; the arrows indicate the increasing direction of the parameter OD.

For the 3 mg particle concentration, results are quite constant in the right part of the cell, only then a slight dispersion is present on the left side (Figure 3a).

The 9 mg particle concentration shows some dispersion even very close to the laser entrance, always increasing while moving to the left (Figure 3b).

The 27 mg concentration shows larger dispersion (Figure 3c).

The results show constant and monotone trends and are not randomly dispersed, which means that the studied parameters are acting on the final results with specific effects.

It is evident that for the low particle concentration, result dispersion is very low, and nearly independent on the optical depth. When increasing the concentration,

the average measured SMD changes with the optical depth and its dispersion increases.

It is also evident that the deviation from the constant ideal value has a systematic behaviour error due to the particle density, since the SMD for the three cells is not the same even at  $OD=0$ , when the laser sheet is directly visible to the camera without attenuation; probably because also the light scattered by the particles beyond the laser sheet are contributing to the signals, and not only those laying between the laser sheet and the CCD camera.

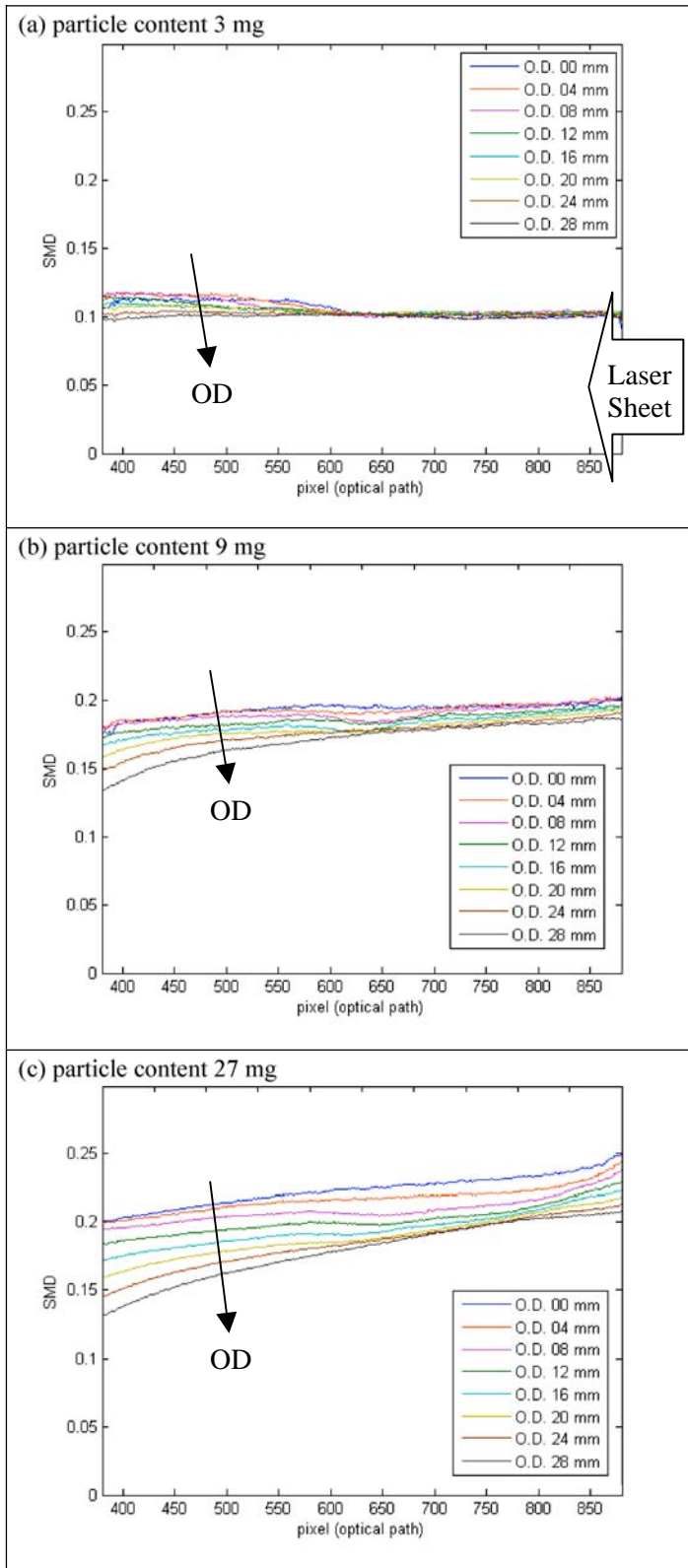


Figure 3 - SMD (a.u.) vs. optical path, varying the optical depth, for the three particle concentrations. The laser sheet is entering from right to left

The results confirm the practical rule given by [8] saying that:

- For extinction coefficient less than 0.1, multiple scattering does not occur or its effects are negligible
- For extinction coefficient between 0.1 and 0.4, multiple scattering does occur and could be a problem
- For extinction coefficient larger than 0.4 multiple scattering occur strongly .

## PDS HYPOTHESES DISCUSSION

In this paragraph the hypotheses that stand on the basis of the PDS technique are analysed and commented, with many remarks issued from the performed work. Comments are subdivided in groups for a single and a group of particles.

### Hypothesis for a single particle

Mie scattering is proportional to the droplet surface.  $S_{Mie} \propto D^2$ . This affirmation is valid in the range of particles larger than the light wavelength [8]. Also the optical density of the particle, which is related to the material optical transmittivity at the considered wavelength and to the particle size, plays a role. For a perfectly transparent material, considering all the infinite scattering orders, all the incident energy is refracted, so that Mie scattering is proportional to  $D^2$ . Also for a perfectly opaque particle, only the reflected radiation would be present and still proportional to  $D^2$ . For a material with a finite attenuation, the amount of energy absorbed and not refracted is influenced by the path length inside the particle, so that for the very small particles nearly all the dominant refraction order would be still present, while for larger particles high order scattering would result attenuated, until only reflection is left for very large particles. In the PDS it is normally considered that droplets are perfectly or nearly transparent to the incident wavelength, and to our knowledge up to now this issue was never considered a problem. Note that if fluorescence happens, some of the incident energy has been used, so for sure a small deviation from the exponent 2 exists. [5] found an exponent 1.975 in their simulation at  $90^\circ$ .

Fluorescent emission is proportional to the droplet volume.  $S_{LIF} \propto D^3$ . This is valid if the particle is transparent to both the exciting and emitted wavelength. If not, the internal part of the particle will not fully participate to the outward emission. This fact will always happen at a certain large dimension, and only the emission coming from a given layer of superficial material will reach the outside, so fluorescence will become proportional to  $D^2$  instead of  $D^3$ , and the PDS cannot be applied. It is not excluded that there could be a lucky combination of attenuation coefficients and particle size that keeps the same signals ratio, but that study is not the aim of the present analysis. [5] made an accurate simulation to find the dye concentration limit and maximum droplet size for the relation to be valid.

The collected signals are constant fractions of the emitted energy. This is a hypothesis that is implicitly done by many authors. Even if it is verified that  $S_{Mie} \propto D^2$  and  $S_{LIF} \propto D^3$ , with the energy integrated over the full  $4\pi$  solid angle, when the ratio of the two measured signals is considered, the radiation is collected by an instrument that integrates over a small solid angle, and each pixel of a CCD camera is a different instrument, because of its slightly different optical path.

In many works it was not found a clear separation between the total emitted radiation  $S_{Mie}$  or  $S_{LIF}$ , and the measured radiation  $I_{Mie}$  or  $I_{LIF}$ , so that  $S = C_1 D^n$  and  $I = C_2 D^n$  are improperly used with the same  $C$  constant.

For example [9] uses a  $C_{LIF}$  and  $C_{Mie}$  as image system constants that seem to be implicitly considered constant for all the pixels.

### Hypotheses for a cloud of particles

Secondary or multiple scattering can be neglected. This is probably the more dangerous hypothesis. To better clarify what is happening, the effects of multiple scattering should be divided into two groups. The first one regarding the signal directed from the visualised particle toward the CCD, and that is partially re-scattered in other directions by other particles found along its path: this decreases the received light. At the same time, light originally directed outside of the CCD is in the same way re-scattered but directed toward the CCD, this increases the signal.

Attenuation of the Mie and LIF signals is the same. This is basically true, since the signal attenuation is mostly due in both cases to other particles encountered along the signal path. A slight difference can arise only from the different attenuation on the two wavelengths in the near forward direction

Increase of the Mie and LIF signals by multiple scattering is the same. This is not possible, since LIF emission is homogeneous, while Mie scattering is strongly directional, and is the major problem of the technique.

[10] simulated a homogeneous spray illuminated only in an isolated square sheet, instead of the experimental sheet that is infinite in the laser propagation direction. In this way he could simulate the image visualised by a traditional camera with a given geometry, and was able to separate the contribution of different scattering orders. The total image shows that the light spreads from the illuminated square toward the same propagation direction of the laser sheet, and that the second order scattering is the main responsible of this spreading. Because of the multiple scattering, the laser sheet spreads with a widening angle while it propagates, and the effect is also that the light intensity is higher on the exit side of the illuminated square sheet.

A clear differentiation of the two phenomena should then state that  $I_{LIF} = C_{LIF} * \Sigma D_i^3$ ,  $I_{Mie} = (C_{Mie1} + C_{Mie2}) * \Sigma D_i^2$  where  $C_{LIF} \propto C_{Mie1}$ , but not  $C_{Mie2}$  that is the additional contribution from secondary scatter, i.e. the part of incident laser that after primary scattering would be directed outside of the receiving optics, but is then redirected toward the optic by other particles. So  $C_{Mie2}$  depends not only on the set-up geometry, but also on the presence of droplet outside of the measured region. The approximation often used is in fact that  $C_{Mie2} = 0$ .

## CONCLUSIONS

A test with monodispersed particles was used to assess the accuracy of the Planar Droplet Sizing technique. The results clearly show that only for a condition of limited particle concentration, that is of optical thickness, the technique can be applied as is; when the optical thickness increases the secondary scattering of incident lights from the particles all over the illuminated suspension is no more negligible, and leads to large systematic errors.

## FUTURE WORK

A method to measure and correct the multiple scattering is proposed in [16], based on the use of a laser beam instead of a sheet, that allows the measure and subtraction of the secondary scattering. A similar concept, with different hypotheses and no experimental results reported, had also been formulated in [17].

The experimental arrangement used showed a strong potential for measurement technique investigation and can be used in various experiments; microspheres of different diameters can be mixed with the desired proportions, so that the accuracy and behaviour of different instruments, like PDA or diffraction instruments, could be tested.

## ACKNOWLEDGMENT

The investigation was financed by “Secretaría de Estado de Universidades e Investigación del Ministerio de Educación y Ciencia, España” (University and Research State Secretary, Spanish Minister of Education and Science). The authors would like to thank Eng. Daniele Carboni for his precious assistance in the laboratory.

## REFERENCES

1. Albrecht, H.-E., Damaschke, N., Borys, M., Tropea, C., Laser Doppler and Phase Doppler Measurement Techniques, (Springer, 2003, 978-3-540-67838-0).
2. Dent JC. “A basis for the comparison of various experimental methods for studying spray penetration”. SAE Paper 710571 (1971)
3. J.M. Desantes, R. Payri, F. J. Salvador, A. Gil, “Development and validation of a theoretical model for diesel spray penetration,” FUEL 85, 910-917 (2006).
4. Wenyi Cai, Christopher F. Powell, Yong Yue, Suresh Narayanan, Jin Wanga, Mark W. Tate, Matthew J. Renzi, Alper Ercan, Ernest Fontes, Sol M. Gruner, “Quantitative analysis of highly transient fuel sprays by time-resolved x-radiography,” Applied Physics Letters 83, 8 (2003).
5. R. Domann, Y. Hardalupas, “Evaluation of Planar Droplet Sizing (PDS) Technique,” in Proceedings of the

8th International Conference on Liquid Atomization and Spray Systems, Pasadena, CA, USA, (July 2000).

6. R. Domann, Y. Hardalupas, “Quantitative Measurement of planar Sauter Mean Diameter in sprays using Planar Droplet Sizing”, in Proceedings of the 11th International Symposium on Application of Laser techniques to Fluid Mechanics, Lisbon, Portugal, (July 2002).

7. E. Dan Hirleman, W. D. Bachalo, Philip G. Felton , Liquid Particle Size Measurement Techniques, 2nd Volume, (ASTM International , 1990, 0803114591)

8. Hendrik Christoffel van de Hulst, Light Scattering by Small Particles, (Dover Publications, New York, 1981)

9. M. C. Jermy D.A. Greenhalgh, “Planar dropsizing by elastic and fluorescent scattering in sprays too dense for phase Doppler measurements,” Appl. Phys B 71, 703-710 (2000)

10. Mark C Jermy and Andrew Allen, “Simulating the effects of multiple scattering on images of dense sprays and particle fields,” Applied Optics, 41, 20, (2002)

11. Sangon Park, Hoon Cho, Ilhan Yoon and Kyoungdoug Min, “Measurement of droplet size distribution of gasoline direct injection spray by droplet generator and planar image technique,” Meas. Sci. Technol. 13, 859–864, (2002).

12. J W Powell, C F Lee, “An Investigation of Multiple Scattering in a Hollow-Cone Spray,” SAE paper 2007-01-0648 (2007).

13. Julian M. Tishkoff, Robert D. Ingebo, Jan B. Kennedy, Liquid Particle Size Measurement Techniques. (ASTM STP 848 , 1984)

14. Renliang Xu, Particle Characterization: light scattering methods, (Kluwer Academic Publishers, ISBN 0-7923-6300-0, 2000)

15. C. N. Yeh, T. Kamimoto, S. Kobori, H. Kosaka: Trans. JSME 93-0134, 308 (1993)

16 José V. Pastor, Raúl Payri, Lucio Araneo, and Julien Manin “Correction method for Droplet Sizing by Laser-Induced Fluorescence in a controlled test situation”, accepted for publication, Journal Optical Engineering, (2008)

17 D. Talley, V. Mcdonell, S. Samuelsen; “Optical Patterning Method”, United States Patent 6734965 (2004).

## LIST OF SYMBOLS

$C_{Mie}$	Optical constant for elastic (Mie) scattering
$C_{LIF}$	Optical constant for fluorescent emission
$D, D_i$	particle or droplet diameter
$I_{Mie}$	intensity of the elastically scattered radiation received by the instrument
$I_{LIF}$	intensity of the fluorescent radiation received by the instrument
OD	Optical depth, thickness of water between laser sheet and camera
PDS	Planar Droplet Sizing
pix	Optical path, measured in pixels along the laser propagation direction
$Q_{ext}$	Extinction efficiency
SMD	Sauter Mean Diameter
$S_{Mie}$	total elastically scattered radiation (often called scattered)
$S_{LIF}$	total fluorescent scattered radiation (often called emitted)
$\rho$	particle number concentration (particle / m <sup>3</sup> )
$\sigma_{geom}$	particle geometric projected surface = $\pi/4 D^2$
$\tau$	optical thickness, also called optical density